Kim *et al. Microbial Cell Factories* (2025) 24:14
https://doi.org/10.1186/s12934-024-02641-5

Microbial Cell Factories

RESEARCH Open Access

Discovery of 15-deoxynaphthomycins activating the antioxidant NRF2-ARE pathway from *Streptomyces* sp. N50 via genome mining, global regulator introduction, and molecular networking

Min-Seon Kim[1†], Baskar Selvaraj[2†], Hee-Tae Yeo[1], Jun-Su Park[1], Jae Wook Lee[2,3*] and Jin-Soo Park[1,3*]

Abstract

Genome mining is a promising avenue for expanding the repertoire of microbial natural products, which are important for drug development. This approach involves predicting genetically encoded small molecules by examining bacterial genomes via accumulated knowledge of microbial biosynthesis. However, it is also important that the microbes produce the predicted molecule in practice. Here, we introduce an endophytic *Streptomyces* sp. N50, which was isolated from the medicinal plant *Selaginella tamariscina*. Upon sequencing its entire genome, 33 biosynthetic gene clusters (BGCs) were identified in a chromosome and a megaplasmid. Subsequent genome mining revealed that the new 15-deoxynaphthomycin could be produced due to the presence of an enoyl reductase domain, which is absent in the known BGC of naphthomycin, a type of ansamycin antibiotics. In addition, the engineered strain with the introduction of the global regulatory gene *afsR2* into N50 successfully produced 15-deoxynaphthomycins. Furthermore, molecular network analysis via MS/MS selectively confirmed the presence of additional sulfur-containing 15-deoxynaphthomycin congeners. Eventually, six new 15-deoxynaphthomycins were isolated and elucidated from the engineered strain N50. This family of compounds is known to exhibit various biological activities. Also, the presence of quinone moieties in these compounds, which are known to activate NRF2, they were tested for their ability to activate NRF2. Among the new compounds, three (1, 5, and 6) activated the antioxidant NRF2-ARE signaling pathway. Treatment with these compounds significantly elevated NRF2 levels in HepG2 cells and further induced the expression of NRF2 target genes associated with the antioxidant response. This study suggests that the combination of genome mining, gene engineering

[†]Min-Seon Kim and Baskar Selvaraj contributed equally to this work.

*Correspondence:
Jae Wook Lee
jwlee5@kist.re.kr
Jin-Soo Park
jinsoopark@kist.re.kr

Full list of author information is available at the end of the article

and molecular networking is helpful for generating new small molecules as pharmaceutical candidates from microorganisms.

Keywords 15-deoxynaphthomycins, NRF2 activator, Genome mining, Molecular networking, Global regulator

Introduction

For decades, natural products have served as an essential starting point in drug discovery and development. Many antimicrobials and chemotherapeutics that have advanced to clinical trials are based on natural products, including primary or secondary metabolites derived from diverse living organisms [24, 44]. Among these sources, *Streptomyces*, the largest genus of Actinobacteria, has been recognized as a prominent producer of valuable small molecules widely used in medicine [40, 60].

Despite the significant contributions of natural products, the development of new drugs from natural products has undergone a noticeable decline in recent years. This reduction can be attributed, in part, to the challenges associated with reisolating known compounds and, more prominently, the enormous costs involved in drug development [1]. To address these pressing issues and reignite drug discovery from natural products, the genome mining approach has emerged as a promising and valuable technique [4, 7, 10]. This approach provides relatively effective tools for identifying unknown biosynthesis-related gene clusters and their products. By harnessing the potential of genome mining, researchers aim to overcome the barriers of compound rediscovery and streamline the process of discovering novel bioactive compounds from microorganisms.

Although genome mining has enabled the prediction of a variety of novel metabolites in microbes, it has not led to their actual production in many cases. This is due to the cryptic or silent states of many biosynthetic gene clusters (BGCs) in laboratory cultures, thus requiring artificial activation of BGCs, such as cocultivation for interspecies crosstalk, chemical elicitor treatment, ribosomal engineering, and the introduction of regulatory genes [65, 45, 52], .

In addition to advances in genome mining and the activation of BGCs, several other cutting-edge techniques are being introduced to explore new secondary metabolites, thus expanding the chemical diversity in drug discovery. One particularly intriguing avenue of exploration involves the study of endophytic bacteria, which are anticipated to biosynthesize new metabolites while maintaining symbiotic relationships with plants [16, 21, 23]. Additionally, researchers are increasingly incorporating molecular network approaches that facilitate the rapid discovery of specific chemical skeletons through MS/MS-based mass spectrometry [33, 49].

In this study, we focused on *Streptomyces* sp. N50, an endophytic bacterium isolated from *Selaginella tamariscina*, a plant known for its use in herbal medicine on the basis of pharmacological research [3, 31]. By combining genome mining with the introduction of the global positive regulatory gene *afsR2* [57], we successfully predicted and activated the biosynthesis of previously unknown 15-deoxynaphthomycins. Moreover, molecular network analysis selectively identified sulfur-harboring derivatives, highlighting the potential of this approach to uncover six structurally diverse 15-deoxynaphthomycins (**1**–**6**). Naphthomycins are potent antimicrobial secondary metabolites derived from *Streptomyces*, belonging to the ansamycin antibiotic family, which is characterized by a rigid aromatic chromophore, making them valuable candidates for advancing antibiotic-related research. The naphthoquinone plumbagin, and naphthomycinol shows significant neuroprotection in Alzheimer's and glutamate neurotoxicity by activating anti-oxidant NRF2 pathway [34, 41]. These molecules contain a quinone moiety, which is known to activate the antioxidant NRF2-ARE signaling pathway. Therefore, we further assessed the ability of these molecules to activate pathways in the HepG2 cell line originated from human liver cancer. The NRF2-ARE pathway is a well-conserved mechanism that helps cells combat oxidative stress [8, 38]. NRF2 is a transcription factor that binds to AREs in promoters, thereby activating the expression of cytoprotective genes. When cells undergo oxidative stress, whether through intra- or extracellular mediators, NRF2-ARE signaling is activated to detoxify and protect them. As a result, compounds **1**, **5**, and **6** significantly increased the NRF2 levels and the expression of NRF2 target genes associated with antioxidant mechanisms.

Materials and methods

Collection and isolation of strains

Endophytic bacteria were isolated from the entire plant of *S. tamariscina* collected on Mt. Nochu in Gangwon-do, Korea (37°32′41.9″N, 128°47′20.4″E). The plant samples were carefully excised and subjected to surface sterilization via sequential treatments of 2% sodium hypochlorite for 30 s and 70% ethanol for 1 h. The plants were subsequently ground and spread onto agar plates containing 20 μg/mL nalidixic acid, 50 μg/mL nystatin, or 50 μg/mL polymyxin B. Following incubation at 27 °C for 2 weeks, diverse colonies emerged on the media. Colonies exhibiting representative actinomycete morphologies were isolated selectively. These isolated strains, including strain N50, were subjected to repeated streaking to achieve

pure cultures, which were then stored at -80 °C for further research purposes.

Genome sequencing, assembly, annotation and bioinformatics analysis

The strain N50 was cultivated in tryptic soy broth medium (BD, Sparks, MD, USA) for three days at 27 °C. The genomic DNA was isolated via a genomic DNA purification kit (Qiagen, Hilden, Germany), and 16 S rRNA PCR was performed via the 16 S rRNA primer pair 27f and 1492r with HiPi Plus (Elpis-Biotech, Daejeon, Republic of Korea). Whole-genome sequencing was performed via a third-generation Pacific Biosciences (PacBio) RSII sequencing system by Macrogen Corporation (Seoul, Republic of Korea).

The reads obtained from the sequencing were assembled via the Hierarchical Genome Assembly Process (HGAP v3.0) [11]. To assess the completeness of the genome assembly, we analyzed the Actinobacteria (odb9) dataset of Benchmarking Universal Single-Copy Orthologs (BUSCO v3.0.2) [55]. For genome annotation, Prokka (v1.13) [53] was utilized, and RNA genes were predicted via RNAmmer (v1.2) [36]. To visualize genomic features, predicted genes, and the distribution of biosynthesis-related gene clusters (BGCs), we generated a circular plot via Circa (https://omgenomics.com/circa/). The functional annotation of the predicted genes was conducted via eggNOG-mapper [26]. To identify biosynthesis-related gene clusters, we employed antiSMASH (v5.1.2) [5].

The complete genome sequence of *Streptomyces* sp. N50 was deposited in NCBI GenBank under accession numbers CP137549–CP137550 (BioProject: PRJNA1029240).

Preparation of the N50 mutant for *afsR2* overexpression

To overexpress *afsR2* in strain N50, the DNA sequence corresponding to *afsR2* was amplified from *S. coelicolor* using previously reported primers with restriction enzyme sites of BamHI and XbaI [50]. The amplified PCR product was ligated into the BamHI and XbaI double-digested pSET152 integrative plasmid with the constitutive promoter *ermE** after cloning with pUC19 and sequence confirmation of the *afsR2* gene.

The recombinant pSET152 plasmid containing *afsR2* was transformed into methylase-negative *E. coli* ET12567/pUZ8002 as a conjugal donor. After conjugation between *E. coli* with the expression plasmid and N50, the N50 mutant (N50-afsR2) with the *afsR2* gene in its chromosome was prepared as previously described [48]. The strains, plasmids, and primers used in this study are listed in Table S1.

Identification of secondary metabolites and molecular network analysis

N50 and N50-afsR2 were inoculated in 20 mL–4 L of yeast malt extract (YME; yeast extract, 4 g/L; malt extract, 10 g/L; dextrose, 4 g/L) liquid media and incubated with constant shaking for 7 days at 28 °C. The cultures were then centrifuged at 3800 rpm for 10 min to separate the supernatant and mycelia. The supernatant was extracted via ethyl acetate (EtOAc), and the resulting fractions were collected via evaporation of the solvent. The metabolites in each solvent extract were analyzed via LC–MS on an Agilent Technologies 1200 system coupled with a Quadrupole 6120 (Agilent, Santa Clara, CA, US) using a Phenomenex Luna C18(2) 5 µm (4.6 × 150 mm) column (Phenomenex, Torrance, CA, US). A gradient method with acetonitrile and water (Thermo Fisher Scientific, Waltham, MA, US) was applied (10% acetonitrile and 90% water to 100% acetonitrile and 0% water over a period of 30 min), with a flow rate of 0.7 mL/min.

High-resolution MS/MS (HR-MS/MS) spectra were produced by using a Q Exactive Quadrupole-Orbitrap mass spectrometer (Thermo Fisher Scientific, Waltham, MA, US) with an ACQUITY UPLC BEH 1.7 µm C18 130 Å (2.1 × 100 mm) column (Waters, Milford, MA, US). The LC–MS/MS data obtained from the crude extracts were subsequently converted. mzXML is compatible with the Global Natural Products Social Molecular Networking (GNPS) platform via MSConvert (v3.0.11244). After the data were uploaded to the GNPS server via the FTP client WinSCP, molecular networks were generated on the GNPS analysis platform, including a filtration step. This step involved the exclusion of all MS/MS fragment ions within a ± 17 Da range of the precursor m/z value. The precursor ion mass tolerance was set to 2.0 Da, and the MS/MS fragment ion tolerance was set to 0.5 Da [59]. To visualize these networks, we utilized Cytoscape (v3.8.2) [54]. This allowed us to explore and analyze the interconnected molecular relationships among the metabolites, providing a comprehensive overview of the chemical diversity present in the crude extracts of N50.

Isolation and structural elucidation of compounds 1–6

Compounds **1–6** were isolated via preparative HPLC (Gilson 321 HPLC system (Gilson, Madison, WI, US)/ column: Phenomenex Luna 10 µm C18(2) (250 × 10 mm) (Phenomenex, Torrance, CA, US), flow rate 4 ml/min) under flow conditions. Conditions for compounds **1–2** from the EtOAc fraction – 38%: 62% acetonitrile: water (30 min isocratic), for compound **3** from the water fraction – 30%: 70% – 50%: 50% (40 min gradient), for compound **4** from the EtOAc fraction – 25%: 75% – 60%: 40% (60 min gradient), and for compounds **5–6** from the EtOAc fraction – 42%: 58 – 61%: 39% (60 min gradient).

The structure of the purified compounds was elucidated via analysis of 1D-NMR (^{1}H and ^{13}C) and 2D-NMR (COSY, HSQC, HMBC, and ROESY) spectra via a 500 MHz Bruker Avance NEO spectrometer equipped with a 5 mm CPP BBO probe (Bruker, Billerica, MA, US).

Bioassay of NRF2-ARE signaling pathway activation by 15-deoxynaphthomycins

Reagents and chemicals

The cell culture media MEM-EBBS (Cytiva, Marlborough, MA, US), fetal bovine serum (Corning, Corning, NY, US), penicillin/streptomycin (Gibco, Grand Island, NY, US), sodium pyruvate (Welgene, Gyeongsan, Republic of Korea), and nonessential amino acids (Welgene, Gyeongsan, Republic of Korea) were used, and the antibodies against NRF2 (12721 S), GAPDH (2118 S), α-tubulin (2125 S), and anti-rabbit IgG HRP-linked antibody (7074 S) were purchased from Cell Signaling Technology (CST, Danvers, MA, USA). TRIzol (Ambion, Austin, TX, US) reagent was used to isolate total RNA, and cDNA was synthesized via Accupower Cycle Script RT Premix (dT20) (Bioneer, Daejon, Republic of Korea) and SYBR Green Master Mix (Bioneer, Daejon, Republic of Korea).

ONE-Glo luciferase assay

HepG2 cells were transiently transfected with the ARE-luciferase vector in 96-well plates (Greiner Bio-One, Kremsmünster, Austria) and incubated for 24 h at 37 °C in a 5% CO_2 incubator [27]. The compounds were then treated directly and incubated for 24 h at 37 °C and 5% CO_2. Then, 50 µL of ONE-Glo reagent (Promega, Madison, WI, US), which was diluted fivefold with water, was added to each well. After 5 min, the luminescence reading was taken with a GloMax navigator (Promega, Madison, WI, US).

Western blot analysis

HepG2 cells (8×10^5) were seeded in a 6-well plate (Corning, Corning, NY, USA). After overnight growth, the cells were directly treated with compounds for 4 h. Next, the cells were lysed for 30 min with cell extraction buffer (Invitrogen, Waltham, MA, US) supplemented with a protease inhibitor cocktail (Roche, Basel, Switzerland). Then, the tubes were centrifuged at 14,000 rpm for 20 min, and the supernatant was collected. The total protein amounts in the lysates were quantified with a BCA assay kit (Thermo Fisher Scientific, Waltham, MA, USA). Then, an equal amount of protein was loaded on an SDS–PAGE gel and resolved at 100 V for 90 min. The proteins were transferred to a PVDF membrane (Merck Millipore, Burlington, MA, US) at 100 V for 90 min. The membranes were blocked with 5% skim milk for 30 min. Primary antibodies were added and incubated overnight at 4 °C with gentle shaking. Then, the secondary antibodies were added and incubated at room temperature for 90 min. Protein bands were developed with West Pico chemiluminescent reagent (Thermo Fisher Scientific, Waltham, MA, US) and imaged with a Fujifilm LAS-3000 imager (Fujifilm, Tokyo, Japan).

NRF2 target gene expression analysis by qPCR

HepG2 cells (8×10^5) were seeded in a 6-well plate (Corning, Corning, NY, USA). After overnight growth, the cells were directly treated with the test compounds for 8 h. Total RNA was subsequently isolated with TRIzol reagent (Ambion, Austin, TX, USA). cDNA was synthesized via an RT premix kit (Bioneer, Daejon, Republic of Korea). The primers used for qPCR were obtained from Bollong MJ et al. [6] (Table S2). qPCR was performed via SYBR Green dye in a Quant Studio 5 Real-Time PCR System (Thermo Fisher Scientific, Waltham, MA, US).

Results

Isolation, genome assembly and annotation of *Streptomyces* sp. N50

The bacterial strain N50 was isolated from the whole body of *S. tamariscina* plants while searching for a strain with a phosphoenolpyruvate mutase-encoding gene (pepM) capable of producing phosphonates (C-P) from plant-associated bacteria. Using C–P selective spectroscopic analyses, including LC–MS/MS and ^{31}P NMR, C–P produced by N50 was identified as known phosphoacetic acid [17]. In pursuit of discovering additional compounds and gaining deeper insights into the genetic potential of N50, whole-genome sequencing was undertaken.

The genome of N50 was sequenced via RSII-type sequencing technology (PacBio) and determined to be 11,551,937 bp from two contigs, including 10,410 coding sequences (CDSs), 32.2% of which were annotated as hypothetical. The contigs were composed of a linear chromosome of 10,079,986 bp (70.2% G + C content) and a linear megaplasmid of 1,471,951 bp (70.0% G + C content). The second contig was designated the megaplasmid for the following reasons: it contains neither tRNA nor rRNA genes [13]; it has only one gene of 24 *Streptomyces*-specific protein-encoding genes found in *S. griseus*, *S. coelicolor*, and *S. avermitilis* [46]. The general features of the two contigs are shown in Fig. 1 and Table S3.

Sequence comparison by 16 S rRNA and average nucleotide identity (ANI) analysis

Phylogenetic analysis of *Streptomyces* sp. N50 was performed by comparing 16 S rRNA gene sequences. As a result, 30 strains of *Streptomyces* species were selected from EzBioCloud (https://www.ezbiocloud.net) based on similarity with 16 S rRNA sequence of the N50. N50 shared the highest 16 S rRNA gene similarity of 99.93%,

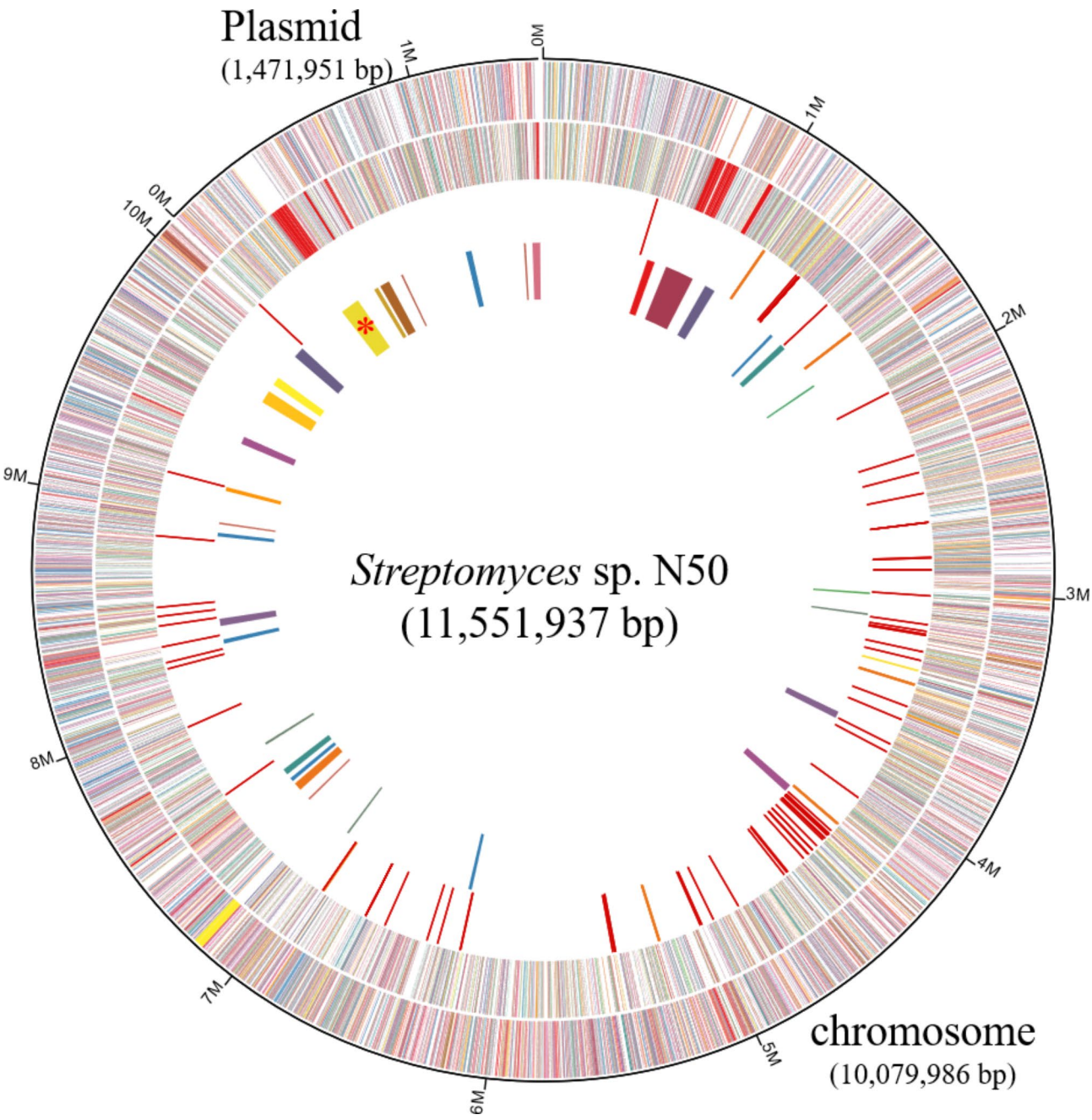

Fig. 1 Schematic representation of the whole genome of strain N50. First/outer ring, size of the genomic sequences in Mbp; second ring. Second and third rings, forward/reverse CDSs colored according to the COG function categories; fourth ring, functional RNA elements (red, tRNA; orange, rRNA; yellow, tmRNA). In the fifth ring, the distribution of secondary metabolic gene clusters is colored to show different product groups, and the BCG for 15-deoxynaphotheomycins is marked with an asterisk

99.79%, and 99.29% with the type strains *S. prunicolor* NBRC 13,075, *S. hokutonensis* R1-NS-10, and *S. graminifolii* JL-22, respectively (Table S4). Recently, average nucleotide identity (ANI) via the whole genome has become a reliable approach for assessing belonging to the same species [29]. ANI analysis was used to evaluate the genetic difference between N50 and its neighbors. Compared with *S. prunicolor*, *S. hokutonensis* and *S. graminifolii* presented ANI values of 92.26%, 90.12%, and 82.99%, respectively. Considering that the species boundary cutoff value is 95–96%, this result suggests that N50 is likely a new species of the genus *Streptomyces*.

Secondary metabolite profiling through genome mining

The genome of N50 was analyzed to estimate its biosynthetic potential to produce secondary metabolites via

the antiSMASH tool [5]. The analysis revealed the presence of a total of 33 BGCs of various types, such as type I polyketides (PKSs), nonribosomal peptides (NRPSs), and terpenes. The products of these BGCs are promising candidates for a variety of bioactive compounds produced by N50. The details of these BGCs are summarized in Table S5, and their distribution in the genome is shown in Fig. 1. The BGC for phosphonoacetic acid that was confirmed to be produced was also identified as 1–19 in Table S5.

Previous studies on Actinobacteria have shown that they harbor diverse giant linear plasmids with critical roles in various aspects of secondary metabolism, such as antibiotic synthesis, degradation of aromatic compounds, and phytopathogenicity. The importance of these plasmids in antibiotic production has been well documented in numerous *Streptomyces* species [35]. Similarly, N50 also carried seven BGCs on the linear plasmid (Table S5). Among them, BGC 2 – 1 stands out because it is located on the plasmid and shares 71% similarity with the naphthomycin BGC from *Streptomyces* sp. CS [61]. This suggested that BGC 2 – 1 may be a unique cluster different from the typical naphthomycin BGC.

Specifically, BCG 2 – 1 consists of 14 modules, each comprising essential components such as ketosynthase (KS), acyltransferase (AT), dehydratase (DH), ketoreductase (KR), and/or enoyl reductase (ER), which are involved in the synthesis of type I polyketide synthase (PKS) products (Table S6, Fig. 2). Compared with the BGC of strain CS, BGC 2 – 1 has an additional ER and an active DH in the 7th module, indicating the production of new naphthomycins, particularly as a structure without the hydroxyl group of C-15. This is highly distinct because more than 15 naphthomycins discovered thus far all contain an OH group at C-15 (Fig. 2) [32, 63, 64].

Activation of the 15-deoxynaphthomycin BGC by the introduction of the global regulatory *afsR2* gene

On the basis of genome mining, N50 was expected to produce small molecules with a 15-deoxynaphthomycin skeleton. To confirm our prediction, culture extracts were prepared from diverse fermentation media and analyzed via LC–MS, but the expected metabolites were

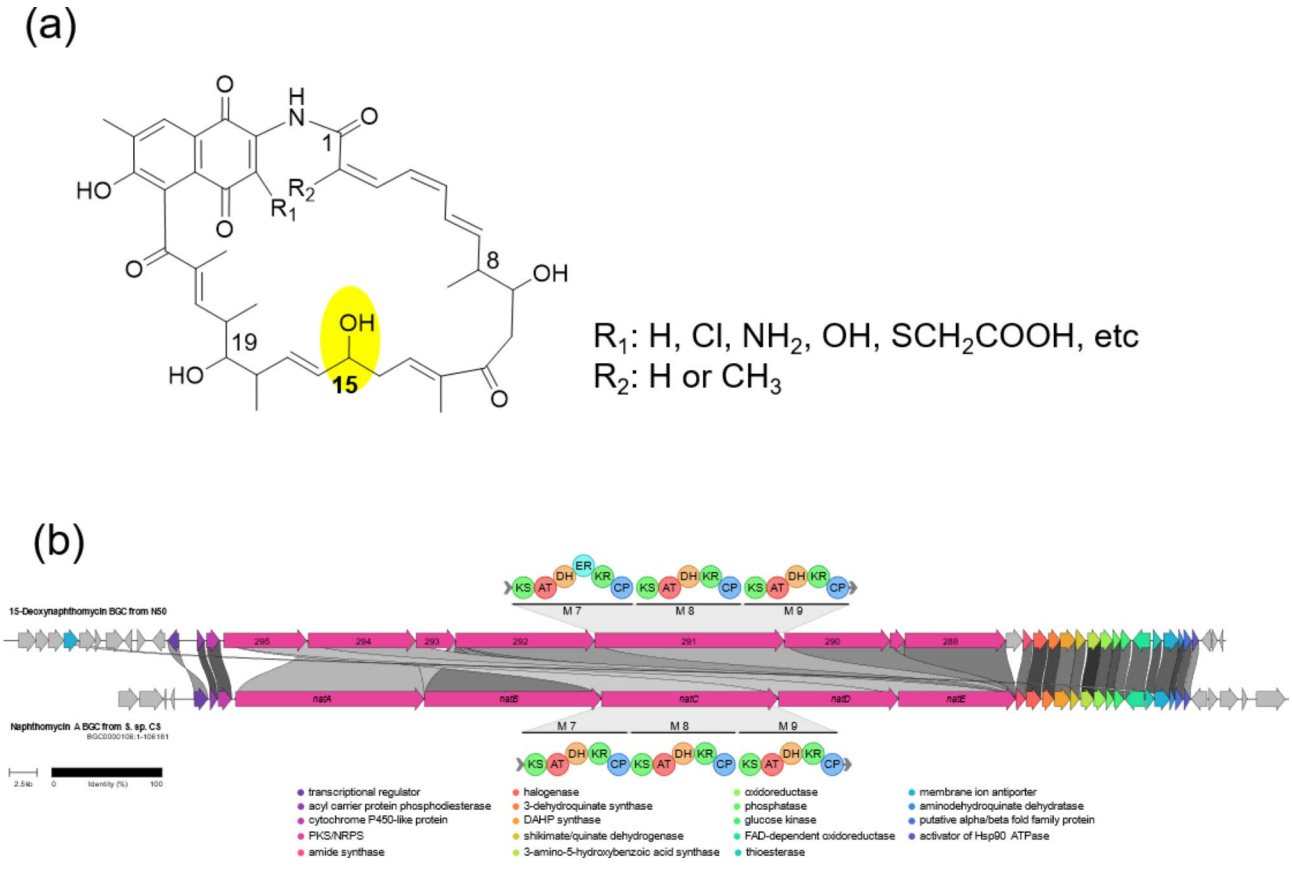

Fig. 2 Structures of the previously reported **(a)** naphthomycin family and **(b)** the BGC of 15-deoxynaphthomycin from *Streptomyces* sp. N50. As highlighted in **(a)**, the previously discovered compounds in the napthomycin family all have a hydroxy group at carbon position 15. The functional DH and ER domains of module 7, as seen in the BGC in **(b)**, allow for the production of 15-deoxynaphthomycin, a fully reduced form at position 15. The BGC comparison between the N50 and Streptomyces sp. CS was prepared using clinker tool [20]

not detected (Fig. 3). Considering that the BGC for 15-deoxynaphthomycin is cryptic, the positive global regulatory gene *afsR2* was introduced into strain N50 via conjugative transformation. According to previous studies, *afsR2* overexpression stimulates the production of bacterial secondary metabolites [37, 50, 57]. The *afsR2* gene was thus amplified from *S. coelicolor*, and the DNA fragment was ligated into the position under the strong promoter *ermE** of the integrative vector pSET152. After conjugation between N50 and *E. coli* harboring the plasmid, the *afsR2* gene was successfully integrated at a single chromosomal site (attB) of the chromosome of N50 by an integrase expressed from pSET152 (Figure S1), yielding the transconjugant carrying the *afsR2* gene. After the mutant was cultured on a small scale (20 mL of YME medium), the solvent extract was analyzed via LC–MS and compared with that of wild-type N50. As shown in Fig. 3, the mutant presented a distinct increase in the production of diverse secondary metabolites.

Molecular network revealing the chemical diversity of 15-deoxynaphthomycins

To determine whether the N50-afsR2 transconjuant is capable of producing deoxynaphthomycins, a list of molecular formulas was prepared by reducing one oxygen in the structure of previously isolated naphthomycins. After HR–MS analysis of the culture extract of N50-afsR2, the presence of these molecules was monitored, and molecular ion peaks ($C_{39}H_{45}O_8NCl$ for $[M+H]^+$) corresponding to naphthomycins B and H ($C_{39}H_{45}O_9NCl$ for $[M+H]^+$) were found. The UV absorption spectrum of the corresponding compound closely resembled those of previously reported naphthomycins, reinforcing its structure. Moreover, the mass spectra revealed that the specific isotope of the compound containing chlorine was identical to that of naphthomycins B and H, further confirming the successful production of the expected metabolite.

Then, via MS2 spectra, a molecular network of the N50 extract was constructed via GNPS, and a partial map containing daughter ions at *m/z* 262 was found in the molecular network. The peak at *m/z* 262 was calculated to contain sulfur ions in naphthoquinone, the chromophore of naphthomycin (Fig. 4). Among previously reported naphthomycins, naphthomycin F and diastovaricin II also harbor a sulfur atom in their structure; thus, the corresponding substances were further separated through preparative HPLC experiments.

Isolation and structural elucidation of 15-deoxynaphthomycins

Preparative chromatography of the gradient solvent system using aqueous acetonitrile yielded a total of six compounds from the ethyl acetate and water fractions. Compound **1** was obtained as a yellow and amorphous powder, and its molecular formula, $C_{39}H_{44}ClNO_8$, was confirmed by HR–MS data after the presence of chlorine was estimated through the isotope pattern of $[M+1]$:

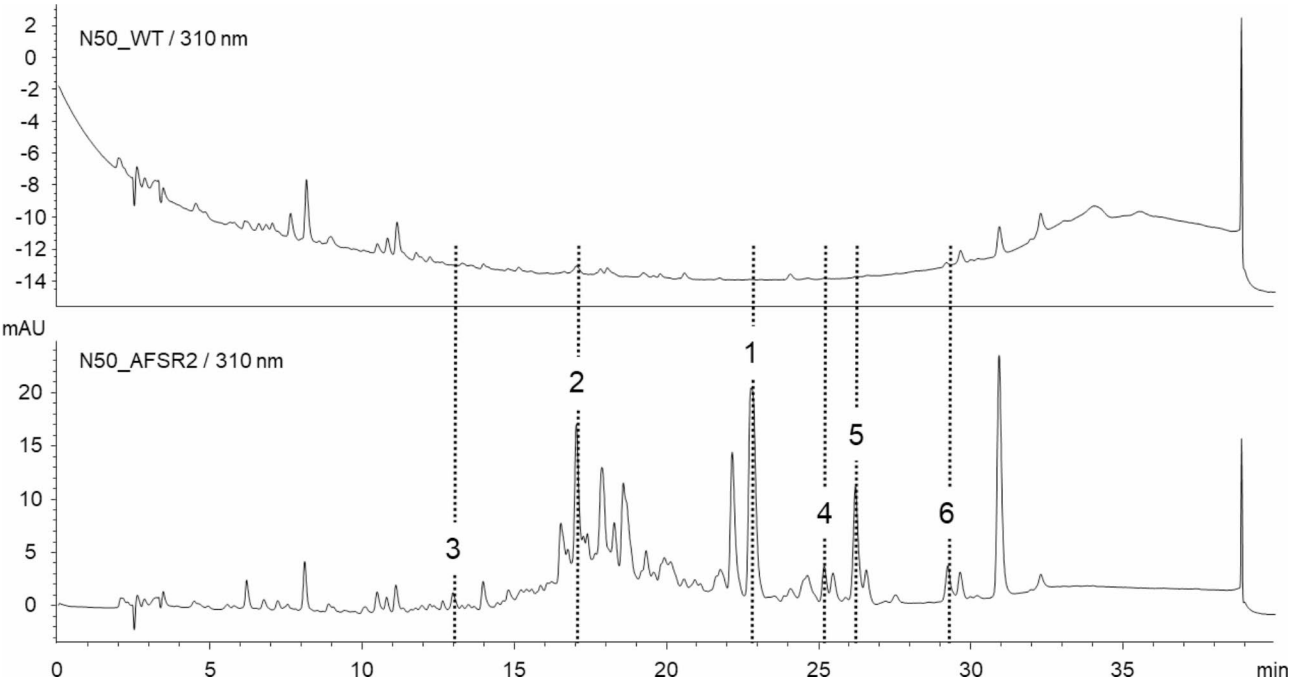

Fig. 3 HPLC chromatograms of N50 (upper) and N50 mutant (bottom) solvent extracts. Each solvent extract was prepared via ethyl acetate after 7 days of incubation in 20 mL of YME medium. The chromatograms were recorded at 310 nm. The six peaks at the dotted positions are the newly identified 15-deoxynaphthomycins

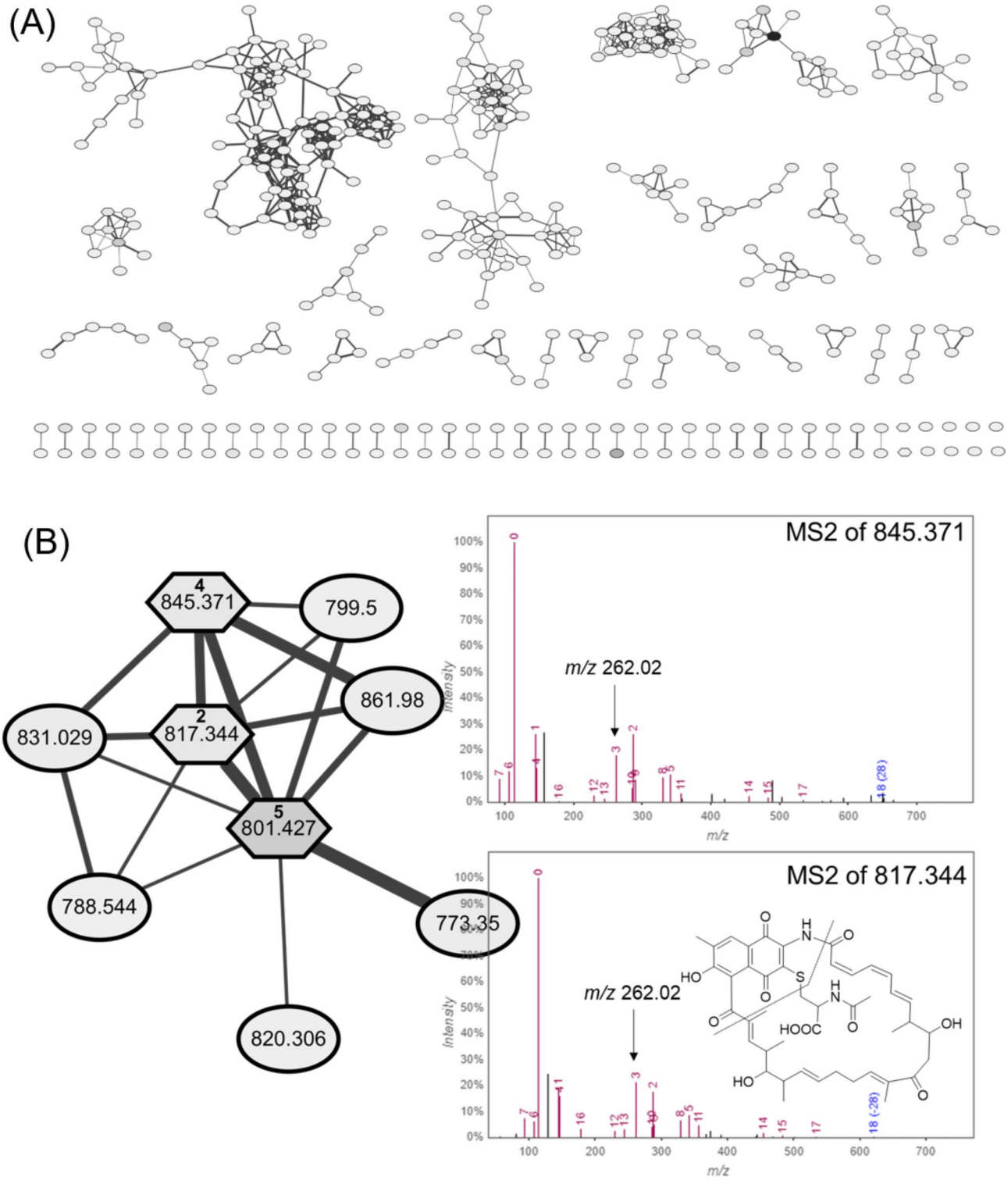

Fig. 4 Molecular networking analysis with the culture extract of *Streptomyces* sp. N50. **(a)** Molecular networks constructed with LC–MS/MS data from the culture extract produced by N50. **(b)** A partial network containing ion 262 indicating a selective naphthoquinone skeleton with a sulfur

[M + 2]: [M + 3] = 5:2:2 in the LC–MS data. In accordance with the molecular formula, 39 carbon resonances were found in the ^{13}C NMR spectrum (Table S7 and Figure S2) and further identified by combined HSQC and HMBC experiments as six methyls, three methylenes, 16 methines, and 14 quaternary carbons (Figures S3-4).

The ^{1}H and ^{13}C NMR spectroscopic data (Table S7 and Figures S1, S5) indicated that **1** closely resembles

previously reported naphthomycins, as expected from BGC analysis. In particular, the NMR data showed high similarities to those of naphthomycins B and H, except for the presence of aliphatic methylene resonances (δ_H 2.10, 2.22) instead of oxygenated methines (δ_{H-15} 4.10 for B and δ_{H-15} 4.04 for H) [39]. 2D NMR experiments, including COSY, HSQC, and HMBC (Figures S3, 4, 6), elucidated the planar structure of **1**, which consisted of two partial polyene-containing structures, C-2 to C-10 and C-12a to C-22a, connected by ^{1}H-^{1}H COSY correlations. Two partial moieties were linked by the HMBC correlations of H-10 (δ_H 2.61, 3.09) and H-12a (δ_H 1.67) with C-11 (δ_C 204.1). The entire planar structure was constructed by further HMBC correlations of H-2 (δ_H 5.92) with C-1 (δ_C 162.0), 29-NH (δ_H 7.93) with C-29 (δ_C 131.0), and H-22a (δ_H 2.03) with C-23 (δ_C 201.8) and C-24 (δ_C 119.7) via 1,4-naphthoquinone, a distinct chromophore of naphthomycins. The double bond configurations of $\Delta_{2,3}$, $\Delta_{4,5}$, $\Delta_{6,7}$, $\Delta_{12,13}$, $\Delta_{16,17}$, and $\Delta_{21,22}$ were determined as Z, Z, E, E, E, and E, respectively, on the basis of vicinal coupling constants ($J_{H-2\&H-3}$= 11.0 Hz, $J_{H-4\&H-5}$= 11.0 Hz, $J_{H-6\&H-7}$=14.7 Hz, and $J_{H-16\&H-17}$ = 15.0 Hz) and ROESY correlations between H-12a (δ_H 1.67 ppm) and H-14 (δ_H 2.11–2.26 ppm) and between H-22a (δ_H 2.03 ppm) and H-20 (δ_H 2.68 ppm) (Fig. 5 and Figure S7). Finally, the structure of **1** was established as chlorine-containing 15-deoxynaphthomycin, as shown in Fig. 5, which was consistent with the interpretation of BGC 2 – 1.

Compound **2** was prepared as an orange solid. The molecular formula of **2** was deduced to be $C_{44}H_{52}N_2O_{11}S$ by HR-ESI-MS, suggesting 20 degrees of unsaturation. A comparison of the 1D NMR spectra (Table S7 and Figure S8) of **2** with those of **1** revealed that **2** also has a 15-deoxynapthomycin skeleton, and the molecular formula difference between **1** and **2** corresponding to $C_5H_8NO_3S$ indicated the modification of chlorine on the naphthoquinone moiety of **1**. Further 2D NMR correlations revealed the existence of *N*-acetylcysteine conjugated with C-30. Specifically, the COSY correlations between H-1' (δ_H 3.36 and 3.23) and H-2' (δ_H 4.51) and the key HMBC correlations from H-2' to C-3' (δ_C 171.5) and C-4' (δ_C 171.6), from H-5' (δ_H 1.85) to C-4', and from H-1' to C30 (δ_C 133.7) confirmed the presence of an *N*-acetylcysteine moiety and its conjugation with the naphthoquinone core structure (Figures S9-11). Accordingly, the structure of **2** was established as shown in Fig. 5.

Among the obtained metabolites, compound **3** was isolated from the water fraction as a yellow solid with a molecular formula of $C_{56}H_{73}N_3O_{20}S$ by HR-ESI-MS. Based on ^{1}H NMR, we recognized **3** as the 15-deoxynaphthomycin scaffold (Table S7 and Figure S12). Like **2**, **3** also has a sulfur atom in its molecular formula, so the presence of an *N*-acetylcysteine moiety was deduced and identified from 2D NMR correlations (Figures S13-15). Apart from the 1D NMR resonances for the 15-deoxynaphthomycin and *N*-acetylcysteine moieties, the signals of six methines were observed [(δ_H 4.11, δ_C 72.0, C-12'), (δ_H 3.35, δ_C 71.8, C-13'), (δ_H 3.59, δ_C 72.5, C-14'), (δ_H 3.16, δ_C 75.0, C-15'), (δ_H 3.70, δ_C 72.7, C-16'), (δ_H 3.46, δ_C 78.7, C-17')], which is typical of an inositol moiety (Fig. 5). In addition, a glucosamine moiety was identified from six methine signals [(δ_H 3.56 and 3.65, δ_C 61.3, C-6'), (δ_H 3.80, δ_C 72.8, C-7'), (δ_H 3.28, δ_C 70.8, C-8'), (δ_H 3.72, δ_C 71.4, C-9'), (δ_H 3.84, δ_C 54.1, C-10')]. These inositol and glucosamine moieties were further constructed by COSY and HMBC correlations (Figures S13-15). This structural analysis confirmed that **3** was formed by substitution of the chlorine in **1** with a mycothiol composed of a cysteine, glucosamine, and inositol, which is the predominant thiol in most species of Actinomycetales [42].

Compound **4** was isolated as an orange solid with the molecular formula $C_{46}H_{56}N_2O_{11}S$, as supported by HR-MS (obsd *m/z* 867.3500, cald m/z 867.3497 for [M + Na]). On the basis of the UV absorption spectrum of **4**, which has λ_{max} values of 234, 286, and 310 nm, similar to those of **1**–**3**, **4** was expected to have a 15-deoxynaphthomycin scaffold, which was verified by the 1D and 2D NMR spectra of **4** (Table S7 and Figures S16–19). The presence of a sulfur atom in the molecular formula of **4** suggested that the modification at C-30 was analogous to that of **2**. Apart from 15-deoxynaphthomycin from C-1 to C-30, the remainder of the molecule was $C_7H_{12}O_3NS$, and the COSY and HMBC correlations confirmed that it was an amide complex between cysteamine and dimethylmalonic acid. Thus, the entire structure of **4** was established as shown in Fig. 5.

Compound **5** was obtained as an orange solid with the molecular formula $C_{45}H_{56}N_2O_9S$ on the basis of HR-MS analysis (obsd *m/z* 823.3597, cald *m/z* 823.3599 for $[M + Na]^+$). The ^{1}H NMR spectrum (Table S7 and Figure S20) of **5** was almost identical to that of **4**, except that **5** was as small as 44 Daltons, indicating CO_2. These data revealed that **5** was the decarboxylated derivative of **4**, and the 2D NMR (Figures S21–23) data also confirmed the decarboxylation of dimethylmalonate to yield the whole structure, as shown in Fig. 5.

Compound **6** was acquired as an orange solid, and its molecular formula was identified as $C_{80}H_{93}N_3O_{16}S$ according to HR-MS analysis (obsd *m/z* 1406.6198, cald *m/z* 1406.6169 for [M + Na]). Although the resolution of the NMR data (Figures S24-27) of **6** was not sufficient to determine the chemical structure because of the small amount compared with the large molecular weight, the spectrum revealed a dimer-like structure of two 15-deoxynaphthomycin scaffolds, which was consistent

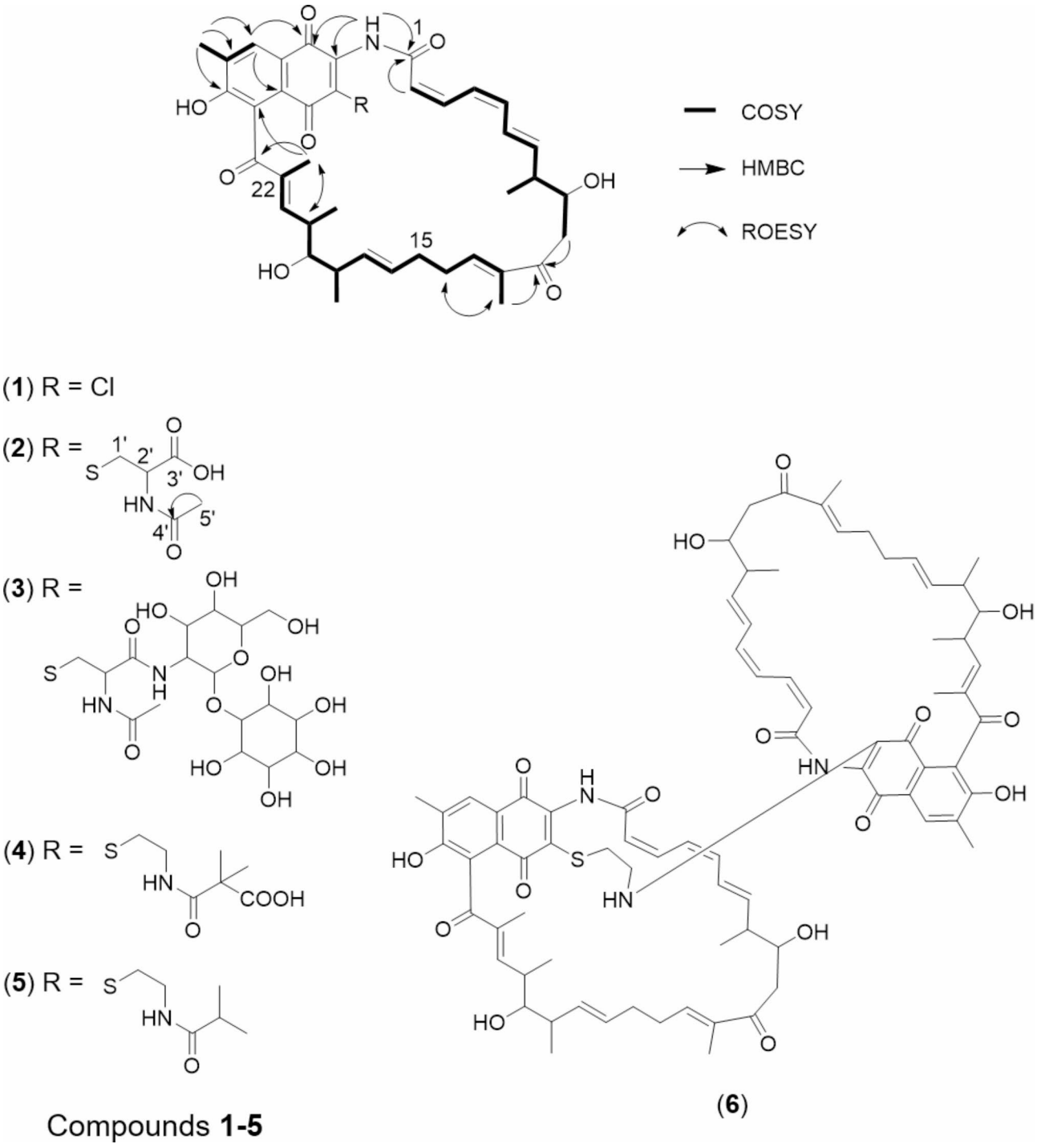

Fig. 5 Chemical structures of 15-deoxynaphthomycins constructed by 1D and 2D NMR experiments, including COSY, key HMBC and ROESY correlations

with the molecular weight being twice that of the other isolated compounds. The structure of **6** was proposed as shown in Fig. 5, and a similar dimer-like molecule of naphthomycin was previously isolated from *Streptomyces* sp. CS [63].

Activation of the NRF2-ARE signaling pathway by 15-deoxynaphthomycins

The NRF2-ARE signaling pathway is associated with protection of cells from excessive oxidative stress-induced damage. It is an intracellular antioxidant defense pathway against oxidative stress [8, 38]. NRF2 is a transcription factor that regulates various cytoprotective genes that

fight against oxidative stress. The genes that are regulated by NRF2 have cis-acting response elements in the promoter called antioxidant response elements (AREs). The NRF2-ARE pathway is also activated by small-molecule drugs and natural compounds [6, 14, 51, 62].

ARE-HepG2 cells were treated with the test compounds for 24 h, and luminescence was measured. The results showed that **1**, **5**, and **6** significantly induced NRF2-ARE-mediated luciferase expression, indicating the activation of the NRF2 signaling pathway (Fig. 6A). Among the three compounds, **1** strongly activated NRF2-ARE mediated luciferase expression 12-fold at 50 µM, **5** activated 6-fold luciferase expression at 16.67 µM, and **6** activated 4-fold luciferase expression at both 5.5 µM and 16.6 µM (Fig. 6A). Further, we performed immunoblotting to confirm the activation of NRF2 by these compounds, and the data revealed that **1**, **5**, and **6** induced the expression of the NRF2 protein in HepG2 cells within 4 h. The data also revealed that **1** strongly increased NRF2 levels, similar to the positive control tBHQ in the immunoblot data (Fig. 6B).

Furthermore, qPCR was performed to assess the ability of activated NRF2 to induce NRF2-ARE target genes associated with the antioxidant pathway. NRF2 regulates the expression of the following cytoprotective genes: heme oxygenase-1 (HO-1), NAD(P)H quinone oxidoreductase 1 (NQO1), thioredoxin reductase 1 (TXNRD1), and glutamate-cysteine ligase (GCLC, GCLM). Once NRF2 is activated, it translocates to the nucleus, binds to AREs, and activates the expression of these genes [62]. The qPCR data revealed increased NRF2 target gene expression after compound treatment for 8 h (Figure S28). The compounds significantly induced NRF2 and its target genes, and among them, **1** activated the NRF2-ARE pathway more significantly than the other compounds did. These 15-deoxynaphthomycins need to be explored further to assess their therapeutic applications.

Discussion

Actinobacteria are known to produce compounds of the ansamycin family, characterized by a macrocycle with a benzenic or naphthalenic chromophore bridged by an aliphatic ansa chain that terminates at the chromophore in an amide linkage [2]. This family includes well-known compounds such as naphthomycin, streptovarcin, rifamycin, geldanamycin, herbimycin, and macbecin, which exhibit various biological activities, including antibacterial, antifungal, antineoplastic, and anticancer effects [39, 47].

In our study, the successful identification of 15-deoxynaphthomycins was achieved by combining the investigation and activation of the BGC in the genome with HR-MS-based metabolite profiling. However, even when genome mining identifies BGCs associated with the production of new compounds, there is no guarantee that these molecules will actually be biosynthesized. As demonstrated in this study, it is necessary to activate biosynthetic pathways through genetic engineering to achieve metabolite production. Moreover, microbes can produce diverse derivatives along with major metabolites. From a medical chemistry perspective, evaluating the bioactivity of all these derivatives is essential. However, minor derivatives are often missed by analytic limitations. Molecular networking has become an effective tool for harvesting these trace molecules. This integrative approach can significantly increase the potential for drug development from natural products.

The literature includes extensive reports of numerous bacterial-derived secondary metabolites containing chlorine or sulfur [22, 30, 58]. It has been hypothesized that sulfur-containing substances among these compounds might originate from mycothiol recycling [28]. Our investigation validated this hypothesis by identifying mycothiol-bound substances, indicating that sulfur compounds are likely generated through this pathway. Mycothiol, a thiol compound abundant in actinobacteria, serves as an analog of glutathione in other bacteria and eukaryotes and is well known for its role in detoxifying external arsenals [43].

NRF2-ARE is a highly conserved endogenous system that protects cells from toxic oxidative stress insults. Previous reports have also demonstrated that several natural products show strong neuroprotective potential by activating the NRF2 signaling pathway both in vitro and in vivo [18, 25, 56]. The isolated compounds were tested for their ability to activate the NRF2-ARE pathway due to the presence of a quinone in their structure. Quinones isolated from plants and bacteria have been widely studied for their neuroprotective effects and NRF2 activity [15]. The quinone family mostly consists of structures such as benzoquinone, naphthoquinone, and anthraquinone. They are present mostly in plants as secondary metabolites [9]. The naphthoquinone plumbagin, which is isolated from *Plumbaginaceae*, provides neuroprotection in Alzheimer's disease mouse models by improving learning and memory via NRF2 activation [41]. Previous reports have revealed that naphthomycinol, which is isolated from *Streptomyces* sp. PF7, is neuroprotective against glutamate-mediated toxicity in neuronal cells [34]. Therefore, we conducted tests using the isolated naphthomycins in HepG2 cells to assess NRF2-ARE activation. Compounds **1**, **3**, and **5** significantly activated NRF2, along with the activation of its target genes HO-1, NQO1, TXNRD1, GCLC, and GCLM. These genes are considered cytoprotective because they facilitate the detoxification of various oxidative stress mediators, such as heme, carbon monoxide, and toxic free radicals, within the cells. In the previous study, napyradiomycins isolated

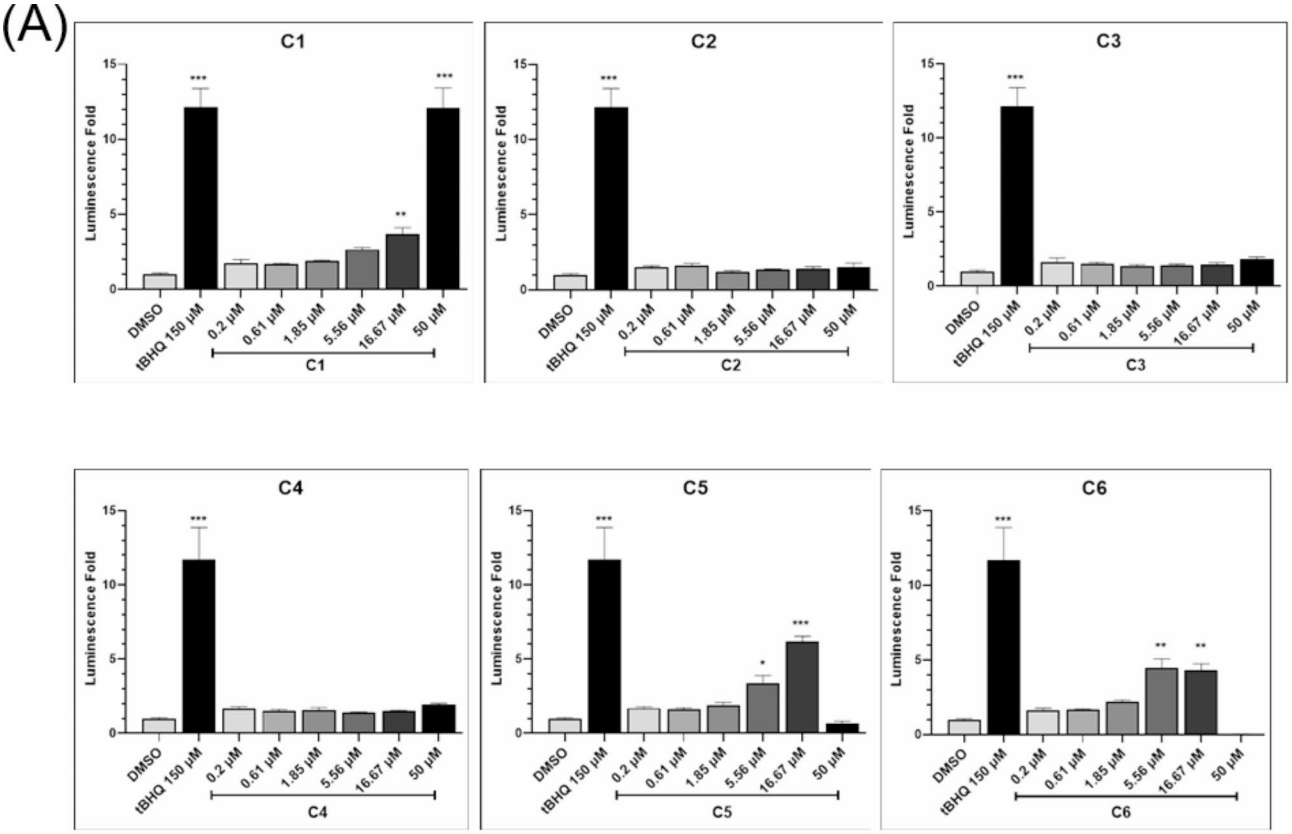

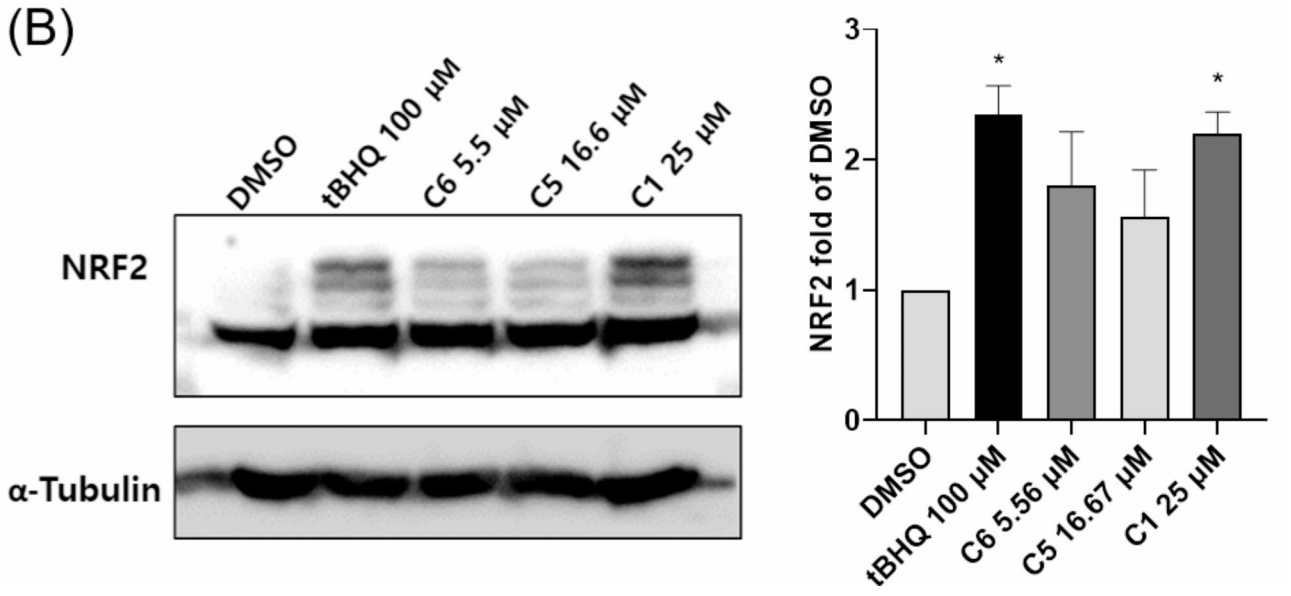

Fig. 6 15-Deoxynaphthomycins activate the ARE-NRF2 signaling pathway. **(a)** The compounds were treated for 24 h, and compounds **1**, **5**, and 6 induced ARE-NRF2-mediated luciferase expression in the ARE-HepG2 reporter cell line. tBHQ (tert-butylhydroquinone) was used as a positive control. Statistical significance: ***$p < 0.001$, **$p < 0.002$, *$p < 0.033$, $N = 2$. **(b)** The compounds increased the NRF2 protein levels. The compounds were treated for 4 h in the HepG2 cell line, and immunoblotting was carried out. Compounds **1**, **5**, and 6 increased NRF2 protein levels, and tBHQ (tert-butylhydroquinone) was used as a positive control. Statistical significance ***$p < 0.001$, **$p < 0.002$, *$p < 0.033$, $N = 2$

from *Streptomyces* sp. YP127 also activated NRF2 and suppressed inflammation in microglia. Napyradiomycins are naphthoquinones with various bioactivities, such as antiapoptotic, antioxidant, and antibacterial potential. 16Z-19-Hydroxynapyradiomycin A1 suppressed the generation of intracellular ROS and the production of inflammatory mediators in activated microglia [12]. Anhydroexfoliamycin reduced neuroinflammation in BV2 cells by inhibiting nuclear factor κB translocation and activating c-jun N-terminal kinase and nitric acid synthase. Additionally, it protects neuronal cells from SHSY-5Y by inducing NRF2 nuclear translocation and reducing intracellular ROS [19]. In this study, we hypothesize that the isolated 15-deoxynaphthomycins might possess significant therapeutic potential against diseases mediated by oxidative stress, and this potential needs to be further explored.

Supplementary Information

The online version contains supplementary material available at https://doi.org/10.1186/s12934-024-02641-5.

Supplementary Material 1

Acknowledgements
This work was supported by the Korea Institute of Science & Technology – Research Programs (2E33301, 2Z07011).

Author contributions
M.S. and B.S. conducted main experiment and H.Y. and J.P.(Jun-Su Park) supported the experiments and discussions. M.S., B.S. and J.P.(Jin-Soo Park) wrote the manuscript. J.L. and J.P.(Jin-Soo Park) conceived and supervised the research. All authors read and approved the final manuscript.

Data availability
No datasets were generated or analysed during the current study.

Declarations

Competing interests
The authors declare no competing interests.

Conflict of interest
The authors declare that they have no competing interests.

Author details
[1]Center for Natural Product Systems Biology, Institute of Natural Product, Korea Institute of Science and Technology, Gangneung 25451, Republic of Korea
[2]Center for Natural Product Efficacy Optimization, Institute of Natural Product, Korea Institute of Science and Technology, Gangneung 25451, Republic of Korea
[3]Natural Product Applied Science, KIST School, University of Science and Technology, Gangneung 25451, Republic of Korea

Received: 4 October 2024 / Accepted: 29 December 2024
Published online: 10 January 2025

References

1 Aigle B, Lautru S, Spiteller D, Dickschat JS, Challis GL, Leblond P, Pernodet J-L. Genome mining of Streptomyces ambofaciens. J Ind Microbiol Biotechnol. 2014;41:251–63. https://doi.org/10.1007/s10295-013-1379-y.
2 August PR, Tang L, Yoon YJ, Ning S, Müller R, Yu T-W, Taylor M, Hoffmann D, Kim C-G, Zhang X. Biosynthesis of the ansamycin antibiotic rifamycin: deductions from the molecular analysis of the Rif biosynthetic gene cluster of Amycolatopsis mediterranei S699. Chem Biol. 1998;5:69–79. https://doi.org/10.1016/S1074-5521(98)90141-7.
3 Bailly C. The traditional and modern uses of Selaginella tamariscina (P.Beauv.) Spring, in medicine and cosmetic: applications and bioactive ingredients. J Ethnopharmacol. 2021;280. https://doi.org/10.1016/j.jep.2021.114444.
4 Bauman KD, Butler KS, Moore BS, Chekan JR. Genome mining methods to discover bioactive natural products. Nat Prod Rep. 2021;38:2100–29. https://doi.org/10.1039/d1np00032b.
5 Blin K, Shaw S, Steinke K, Villebro R, Ziemert N, Lee SY, Medema MH, Weber T. antiSMASH 5.0: updates to the secondary metabolite genome mining pipeline. Nucleic Acids Res. 2019;47:W81–7. https://doi.org/10.1093/nar/gkz310.
6 Bollong MJ, Lee G, Coukos JS, Yun H, Zambaldo C, Chang JW, Chin EN, Ahmad I, Chatterjee AK, Lairson LL, Schultz PG, Moellering RE. A metabolite-derived protein modification integrates glycolysis with KEAP1-NRF2 signalling. Nature. 2018;562:600–4. https://doi.org/10.1038/s41586-018-0622-0.
7 Brinkmann S, Kurz M, Patras MA, Hartwig C, Marner M, Leis B, Billion A, Kleiner Y, Bauer A, Toti L, Pöverlein C, Hammann PE, Vilcinskas A, Glaeser J, Spohn M, Schäberle TF. Genomic and Chemical Decryption of the Bacteroidetes Phylum for its potential to Biosynthesize Natural products. Microbiol Spectr. 2022;10. https://doi.org/10.1128/spectrum.02479-21.
8 Buendia I, Michalska P, Navarro E, Gameiro I, Egea J, Leon R. Nrf2-ARE pathway: an emerging target against oxidative stress and neuroinflammation in neurodegenerative diseases. Pharmacol Ther. 2016;157:84–104. https://doi.org/10.1016/j.pharmthera.2015.11.003.
9 Campora M, Francesconi V, Schenone S, Tasso B, Tonelli M. Journey on Naphthoquinone and Anthraquinone Derivatives: New Insights in Alzheimer's Disease. Pharmaceuticals. 2021;14. https://doi.org/10.3390/ph14010033.
10 Challis GL. Genome mining for novel natural product discovery. J Med Chem. 2008;51:2618–28. https://doi.org/10.1021/jm700948z.
11 Chin CS, Alexander DH, Marks P, Klammer AA, Drake J, Heiner C, Clum A, Copeland A, Huddleston J, Eichler EE, Turner SW, Korlach J. Nonhybrid, finished microbial genome assemblies from long-read SMRT sequencing data. Nat Methods. 2013;10:563–. https://doi.org/10.1038/Nmeth.2474.
12 Choi JW, Kim GJ, Kim HJ, Nam JW, Kim J, Chin J, Park JH, Choi H, Park KD. Identification and evaluation of a napyradiomycin as a potent Nrf2 activator: antioxidative and anti-inflammatory activities. Bioorg Chem. 2020;105. https://doi.org/10.1016/j.bioorg.2020.104434.
13 Claesson MJ, Li Y, Leahy S, Canchaya C, Van Pijkeren JP, Cerdeno-Tarraga AM, Parkhill J, Flynn S, O'sullivan GC, Collins JK, Higgins D, Shanahan F, Fitzgerald GF, Van Sinderen D, O'toole PW. Multireplicon genome architecture of Lactobacillus salivarius. Proc Natl Acad Sci U S A. 2006;103:6718–23. https://doi.org/10.1073/pnas.0511060103.
14 Cores A, Abril S, Michalska P, Duarte P, Olives AI, Martin MA, Villacampa M, Leon R, Menendez JC. Bisavenathramide Analogs as Nrf2 inductors and neuroprotectors in in Vitro models of oxidative stress and hyperphosphorylation. Antioxidants-Basel. 2021;10. https://doi.org/10.3390/antiox10060941.
15 Cores A, Carmona-Zafra N, Clerigue J, Villacampa M, Menendez JC. Quinones as neuroprotective agents. Volume 12. Antioxidants; 2023. p. ARTN. https://doi.org/10.3390/antiox12071464.
16 Dinesh R, Srinivasan V, Te S, Anandaraj M, Srambikkal H. Endophytic actinobacteria: diversity, secondary metabolism and mechanisms to unsilence biosynthetic gene clusters. Crit Rev Microbiol. 2017;43:546–66. https://doi.org/10.1080/1040841X.2016.1270895.
17 Freestone TS, Ju KS, Wang B, Zhao H. Discovery of a Phosphonoacetic Acid Derived Natural product by Pathway Refactoring. ACS Synth Biol. 2017;6:217–23. https://doi.org/10.1021/acssynbio.6b00299.
18 Gao J, Ma C, Xia D, Chen N, Zhang J, Xu F, Li F, He Y, Gong Q. Icariside II preconditioning evokes robust neuroprotection against ischaemic stroke, by targeting Nrf2 and the OXPHOS/NF-kappaB/ferroptosis pathway. Br J Pharmacol. 2023;180:308–29. https://doi.org/10.1111/bph.15961.
19 Gegunde S, Alfonso A, Alvarino R, Perez-Fuentes N, Botana LM. Anhydroexfoliamycin, a Streptomyces secondary metabolite, mitigates Microglia-Driven inflammation. ACS Chem Neurosci. 2021;12:2336–46. https://doi.org/10.1021/acschemneuro.1c00033.

20 Gilchrist CLM, Chooi Y-H. Clinker & clustermap.js: automatic generation of gene cluster comparison figures. Bioinformatics. 2021;37:2473–5. https://doi.org/10.1093/bioinformatics/btab007.

21 Golinska P, Wypij M, Agarkar G, Rathod D, Dahm H, Rai M. Endophytic actinobacteria of medicinal plants: diversity and bioactivity. Antonie Van Leeuwenhoek. 2015;108:267–89. https://doi.org/10.1007/s10482-015-0502-7.

22 Hai Y, Wei MY, Wang CY, Gu YC, Shao CL. The intriguing chemistry and biology of sulfur-containing natural products from marine microorganisms (1987–2020). Mar Life Sci Technol. 2021;3(4):488–518. https://doi.org/10.1007/s42995-021-00101-2.

23 Hardoim PR, Van Overbeek LS, Berg G, Pirttilä AM, Compant S, Campisano A, Döring M, Sessitsch A. The Hidden World within plants: ecological and evolutionary considerations for defining functioning of Microbial endophytes. Microbiol Mol Biol Rev. 2015;79:293–320. https://doi.org/10.1128/Mmbr.00050-14.

24 Harir M, Bendif H, Bellahcene M, Fortas Z, Pogni R. Streptomyces secondary metabolites. Basic Biol Appl Actinobac. 2018;6:99–122. https://doi.org/10.5772/intechopen.79890.

25 Hu QW, Zuo TR, Deng L, Chen S, Liu SW, Liu JD, Wang X, Fan XM, Dong Z. beta-caryophyllene suppresses ferroptosis induced by cerebral ischemia–reperfusion via activation of the NRF2/HO-1 signaling pathway in MCAO/R rats. Phytomedicine. 2022;102. https://doi.org/10.1016/j.phymed.2022.154112.

26 Huerta-Cepas J, Szklarczyk D, Heller D, Hernandez-Plaza A, Forslund SK, Cook H, Mende DR, Letunic I, Rattei T, Jensen LJ, Von Mering C, Bork P. eggNOG 5.0: a hierarchical, functionally and phylogenetically annotated orthology resource based on 5090 organisms and 2502 viruses. Nucleic Acids Res. 2019;47:D309–14. https://doi.org/10.1093/nar/gky1085.

27 Hur W, Sun Z, Jiang T, Mason DE, Peters EC, Zhang DD, Luesch H, Schultz PG, Gray NS. A small-molecule inducer of the antioxidant response element. Chem Biol. 2010;17:537–47. https://doi.org/10.1016/j.chembiol.2010.03.013.

28 Ikeda H, Shin-ya K, Nagamitsu T, Tomoda H. Biosynthesis of mercapturic acid derivative of the labdane-type diterpene, cyslabdan that potentiates imipenem activity against methicillin-resistant *Staphylococcus aureus*: cyslabdan is generated by mycothiol-mediated xenobiotic detoxification. J Ind Microbiol Biot. 2016;43(2–3):325–42. https://doi.org/10.1007/s10295-015-1694-6.

29 Jain C, Rodriguez RL, Phillippy AM, Konstantinidis KT, Aluru S. High throughput ANI analysis of 90K prokaryotic genomes reveals clear species boundaries. Nat Commun. 2018;9:5114. https://doi.org/10.1038/s41467-018-07641-9.

30 Jothivasan VK, Hamilton CJ. Mycothiol: synthesis, biosynthesis and biological functions of the major low molecular weight thiol in actinomycetes. Nat Prod Rep. 2008;25(6):1091–117. https://doi.org/10.1039/b616489g.

31 Jung HJ, Sung WS, Yeo SH, Kim HS, Lee IS, Woo ER, Lee DG. Antifungal effect of amentoflavone derived from. Arch Pharm Res. 2006;29:746–51. doi:Doi 10.1007/Bf02974074.

32 Kang Q, Shen Y, Bai L. Biosynthesis of 3,5-AHBA-derived natural products. Nat Prod Rep. 2012;29:243–63. https://doi.org/10.1039/c2np00019a.

33 Kim D, Hong SC, Yang Y, Choi J, Park JS. Chemical and genomic analyses of a marine-derived Streptomyces sp. V17-9 producing amino acid derivatives and siderophores. Front Mar Sci. 2022;9. https://doi.org/10.3389/fmars.2022.959690.

34 Kim JS, Shin-Ya K, Eishima J, Furihata K, Seto H. A novel neuronal cell protecting substance, naphthomycinol, produced by Streptomyces sp. PF7. J Antibiot (Tokyo). 1996;49:1172–4. https://doi.org/10.7164/antibiotics.49.1172.

35 Kinashi H. Giant linear plasmids in Streptomyces: a treasure trove of antibiotic biosynthetic clusters. J Antibiot (Tokyo). 2011;64:19–25. https://doi.org/10.1038/ja.2010.146.

36 Lagesen K, Hallin P, Rodland EA, Staerfeldt HH, Rognes T, Ussery DW. RNAmmer: consistent and rapid annotation of ribosomal RNA genes. Nucleic Acids Res. 2007;35:3100–8. https://doi.org/10.1093/nar/gkm160.

37 Lee JY, Hwang YS, Kim SS, Kim ES, Choi CY. Effect of a global regulatory gene, afsR2, from Streptomyces lividans on avermectin production in Streptomyces avermitilis. J Biosci Bioeng. 2000;89:606–8. https://doi.org/10.1016/S1389-1723(00)80065-1.

38 Ma Q. Role of nrf2 in oxidative stress and toxicity. Annu Rev Pharmacol Toxicol. 2013;53:401–26. https://doi.org/10.1146/annurev-pharmtox-011112-140320.

39 Mukhopadhyay T, Franco C, Reddy G, Ganguli B, Fehlhaber H. A new ansamycin antibiotic, naphthomycin H from a Streptomyces species Y-83, 40369. J Antibiot. 1985;38:948–51. https://doi.org/10.7164/antibiotics.38.948.

40 Nakaew N, Lumyong S, Sloan WT, Sungthong R. Bioactivities and genome insights of a thermotolerant antibiotics-producing Streptomyces sp. TM32 reveal its potentials for novel drug discovery. MicrobiologyOpen. 2019;8:e842. https://doi.org/10.1002/mbo3.842.

41 Nakhate KT, Bharne AP, Verma VS, Aru DN, Kokare DM. Plumbagin ameliorates memory dysfunction in streptozotocin induced Alzheimer's disease via activation of Nrf2/ARE pathway and inhibition of beta-secretase. Biomed Pharmacother. 2018;101:379–90. https://doi.org/10.1016/j.biopha.2018.02.052.

42 Newton GL, Arnold K, Price MS, Sherrill C, Delcardayre SB, Aharonowitz Y, Cohen G, Davies J, Fahey RC, Davis C. Distribution of thiols in microorganisms: mycothiol is a major thiol in most actinomycetes. J Bacteriol. 1996;178:1990–5. https://doi.org/10.1128/jb.178.7.1990-1995.1996.

43 Newton GL, Buchmeier N, Fahey RC. Biosynthesis and functions of mycothiol, the unique protective thiol of Actinobacteria. Microbiol Mol Biol Rev. 2008;72(3):471–94. https://doi.org/10.1128/MMBR.00008-08.

44 Nguyen HT, Pokhrel AR, Nguyen CT, Dhakal D, Lim HN, Jung HJ, Kim T-S, Yamaguchi T, Sohng JK. Streptomyces sp. VN1, a producer of diverse metabolites including nonnatural furan-type anticancer compound. Sci Rep. 2020;10:1–14. https://doi.org/10.1038/s41598-020-58623-1.

45 Ochi KH, T. New strategies for drug discovery: activation of silent or weakly expressed microbial gene clusters. Appl Microbiol Biotechnol. 2013;97:87–98. https://doi.org/10.1007/s00253-012-4551-9.

46 Ohnishi Y, Ishikawa J, Hara H, Suzuki H, Ikenoya M, Ikeda H, Yamashita A, Hattori M, Horinouchi S. Genome sequence of the streptomycin-producing microorganism Streptomyces griseus IFO 13350. J Bacteriol. 2008;190:4050–60. https://doi.org/10.1128/JB.00204-08.

47 Okabe T, Yuan BD, Isono F, Sato I, Fukazawa H, Nishimura T, Tanaka N. Studies on antineoplastic activity of naphthomycin, a naphthalenic ansamycin, and its mode of action. J Antibiot. 1985;38:230–5. https://doi.org/10.7164/antibiotics.38.230.

48 Paranthaman S, Dharmalingam K. Intergeneric conjugation in Streptomyces peucetius and Streptomyces sp. Strain C5: chromosomal integration and expression of recombinant plasmids carrying the chiC gene. Appl Environ Microb. 2003;69:84–91. https://doi.org/10.1128/Aem.69.1.84-91.2003.

49 Park J-S, Kim D-E, Hong S-C, Kim S-Y, Kwon HC, Hyun C-G, Choi J. Genome analysis of Streptomyces nojiriensis JCM 3382 and distribution of gene clusters for three antibiotics and an azasugar across the Genus Streptomyces. Microorganisms. 2021;9:1802.

50 Park SH, Choi SS, Sherman DH, Kim ES. A global positive regulator afsR2 stimulates tautomycetin production via pathway-specific regulatory gene overexpression in Streptomyces sp. CK4412. Process Biochem. 2009;44:1298–301. https://doi.org/10.1016/j.procbio.2009.08.005.

51 Paudel P, Jung HA, Choi JS. Anthraquinone and naphthopyrone glycosides from Cassia obtusifolia seeds mediate hepatoprotection via Nrf2-mediated HO-1 activation and MAPK modulation. Arch Pharm Res. 2018;41:677–89. https://doi.org/10.1007/s12272-018-1040-4.

52 Rutledge PJ, Challis GL. Discovery of microbial natural products by activation of silent biosynthetic gene clusters. Nat Rev Microbiol. 2015;13:509–23. https://doi.org/10.1038/nrmicro3496.

53 Seemann T. Prokka: rapid prokaryotic genome annotation. Bioinformatics. 2014;30:2068–9. https://doi.org/10.1093/bioinformatics/btu153.

54 Shannon P, Markiel A, Ozier O, Baliga NS, Wang JT, Ramage D, Amin N, Schwikowski B, Ideker T. Cytoscape: a software environment for integrated models of biomolecular interaction networks. Genome Res. 2003;13:2498–504. https://doi.org/10.1101/gr.1239303.

55 Simao FA, Waterhouse RM, Ioannidis P, Kriventseva EV, Zdobnov EM. BUSCO: assessing genome assembly and annotation completeness with single-copy orthologs. Bioinformatics. 2015;31:3210–2. https://doi.org/10.1093/bioinformatics/btv351.

56 Taguchi K, Kensler TW. Nrf2 in liver toxicology. Arch Pharm Res. 2020;43:337–49. https://doi.org/10.1007/s12272-019-01192-3.

57 Vogtli M, Chang PC, Cohen SN. Afsr2 - a previously undetected gene encoding a 63-Amino-acid protein that stimulates antibiotic production in Streptomyces-Lividans. Mol Microbiol. 1994;14:643–53. https://doi.org/10.1111/j.1365-2958.1994.tb01303.x.

58 Wagner C, El Omari M, Konig GM. Biohalogenation: nature's way to synthesize halogenated metabolites. J Nat Prod. 2009;72(3):540–53. https://doi.org/10.1021/np800651m.

59 Wang M, Carver JJ, Phelan VV, Sanchez LM, Garg N, Peng Y, Nguyen DD, Watrous J, Kapono CA, Luzzatto-Knaan T, Porto C, Bouslimani A, Melnik AV, Meehan MJ, Liu WT, Crusemann M, Boudreau PD, Esquenazi E, Sandoval-Calderon M, Kersten RD, Pace LA, Quinn RA, Duncan KR, Hsu CC, Floros DJ, Gavilan RG, Kleigrewe K, Northen T, Dutton RJ, Parrot D, Carlson EE, Aigle B, Michelsen CF, Jelsbak L, Sohlenkamp C, Pevzner P, Edlund A, Mclean J, Piel

J, Murphy BT, Gerwick L, Liaw CC, Yang YL, Humpf HU, Maansson M, Keyzers RA, Sims AC, Johnson AR, Sidebottom AM, Sedio BE, Klitgaard A, Larson CB, Torres-Mendoza PCB, Gonzalez D, Silva DJ, Marques DB, Demarque LM, Pociute DP, O'neill E, Briand EC, Helfrich E, Granatosky EJN, Glukhov EA, Ryffel E, Houson F, Mohimani H, Kharbush H, Zeng JJ, Vorholt Y, Kurita JA, Charusanti KL, Mcphail P, Nielsen KL, Vuong KF, Elfeki L, Traxler M, Engene MF, Koyama N, Vining N, Baric OB, Silva R, Mascuch RR, Tomasi SJ, Jenkins S, Macherla S, Hoffman V, Agarwal T, Williams V, Dai PG, Neupane J, Gurr R, Rodriguez J, Lamsa AMC, Zhang A, Dorrestein C, Duggan K, Almaliti BM, Allard J, Phapale PM P, et al. Sharing and community curation of mass spectrometry data with Global Natural products Social Molecular networking. Nat Biotechnol. 2016;34:828–37. https://doi.org/10.1038/nbt.3597.

60 Watve MG, Tickoo R, Jog MM, Bhole BD. How many antibiotics are produced by the genus? Arch Microbiol. 2001;176:386–90. https://doi.org/10.1007/s002030100345.

61 Wu Y, Kang Q, Shen Y, Su W, Bai L. Cloning and functional analysis of the naphthomycin biosynthetic gene cluster in Streptomyces Sp. CS Mol Biosyst. 2011;7:2459–69. https://doi.org/10.1039/c1mb05036b.

62 Yan J, Pang Y, Zhuang J, Lin H, Zhang Q, Han L, Ke P, Zhuang J, Huang X. Selenepezil, a selenium-containing compound, exerts neuroprotective effect via modulation of the Keap1-Nrf2-ARE pathway and attenuates Abeta-Induced Cognitive impairment in vivo. ACS Chem Neurosci. 2019;10:2903–14. https://doi.org/10.1021/acschemneuro.9b00106.

63 Yang YH, Fu XL, Li LQ, Zeng Y, Li CY, He YN, Zhao PJ. Naphthomycins L-N, ansamycin antibiotics from Streptomyces Sp. CS J Nat Prod. 2012;75:1409–13. https://doi.org/10.1021/np300109s.

64 Yang YH, Yang DS, Li GH, Liu R, Huang XW, Zhang KQ, Zhao PJ. New secondary metabolites from an engineering mutant of endophytic Streptomyces sp. CS Fitoterapia. 2018;130:17–25. https://doi.org/10.1016/j.fitote.2018.07.019.

65 Zhang XF, Hindra, Elliot MA. Unlocking the trove of metabolic treasures: activating silent biosynthetic gene clusters in bacteria and fungi. Curr Opin Microbiol. 2019;51:9–15. https://doi.org/10.1016/j.mib.2019.03.003.

Publisher's note